ONCOLOGY

Preoperative pelvic MRI and 2-[18F]FDG PET/CT for lymph node staging and prognostication in endometrial cancer—time to revisit current imaging guidelines?

Kristine E. Fasmer [1,2] • Ankush Gulati [1,2] • Julie A. Dybvik [1,2] • Kari S. Wagner-Larsen [1,2] • Njål Lura [1,2] •
Øyvind Salvesen [3] • David Forsse [4,5] • Jone Trovik [4,5] • Johanna M. A. Pijnenborg [6] • Camilla Krakstad [4,5] •
Ingfrid S. Haldorsen [1,2]

Abstract

Objective This study presents the diagnostic performance of four different preoperative imaging workups (IWs) for prediction of lymph node metastases (LNMs) in endometrial cancer (EC): pelvic MRI alone (IW1), MRI and [18F]FDG-PET/CT in all patients (IW2), MRI with selective [18F]FDG-PET/CT if high-risk preoperative histology (IW3), and MRI with selective [18F]FDG-PET/CT if MRI indicates FIGO stage ≥ 1B (IW4).

Methods In 361 EC patients, preoperative staging parameters from both pelvic MRI and [18F]FDG-PET/CT were recorded. Area under receiver operating characteristic curves (ROC AUC) compared the diagnostic performance for the different imaging parameters and workups for predicting surgicopathological FIGO stage. Survival data were assessed using Kaplan-Meier estimator with log-rank test.

Results MRI and [18F]FDG-PET/CT staging parameters yielded similar AUCs for predicting corresponding FIGO staging parameters in low-risk versus high-risk histology groups ($p \geq 0.16$). The sensitivities, specificities, and AUCs for LNM prediction were as follows: IW1—33% [9/27], 95% [185/193], and 0.64; IW2—56% [15/27], 90% [174/193], and 0.73 ($p = 0.04$ vs. IW1); IW3—44% [12/27], 94% [181/193], and 0.69 ($p = 0.13$ vs. IW1); and IW4—52% [14/27], 91% [176/193], and 0.72 ($p = 0.06$ vs. IW1). IW3 and IW4 selected 34% [121/361] and 54% [194/361] to [18F]FDG-PET/CT, respectively. Employing IW4 identified three distinct patient risk groups that exhibited increasing FIGO stage ($p < 0.001$) and stepwise reductions in survival ($p \leq 0.002$).

Conclusion Selective [18F]FDG-PET/CT in patients with high-risk MRI findings yields better detection of LNM than MRI alone, and similar diagnostic performance to that of MRI and [18F]FDG-PET/CT in all.

Key Points

• *Imaging by MRI and [18F]FDG PET/CT yields similar diagnostic performance in low- and high-risk histology groups for predicting central FIGO staging parameters.*

• *Utilizing a stepwise imaging workup with MRI in all patients and [18F]FDG-PET/CT in selected patients based on MRI findings identifies preoperative risk groups exhibiting significantly different survival.*

• *The proposed imaging workup selecting ~54% of the patients to [18F]FDG-PET/CT yield better detection of LNMs than MRI alone, and similar LNM detection to that of MRI and [18F]FDG-PET/CT in all.*

✉ Kristine E. Fasmer
kristine.fasmer@helse-bergen.no

✉ Ingfrid S. Haldorsen
ingfrid.haldorsen@helse-bergen.no

[1] Mohn Medical Imaging and Visualization Centre (MMIV), Department of Radiology, Haukeland University Hospital, Bergen, Norway

[2] Section for Radiology, Department of Clinical Medicine, University of Bergen, Bergen, Norway

[3] Unit for applied Clinical Research, Department of Public Health and Nursing, Norwegian University of Science and Technology, Trondheim, Norway

[4] Department of Obstetrics and Gynaecology, Haukeland University Hospital, Bergen, Norway

[5] Centre for Cancer Biomarkers, Department of Clinical Science, University of Bergen, Bergen, Norway

[6] Department of Obstetrics and Gynaecology, Radboud University Medical Center, Nijmegen, The Netherlands

Springer

Abbreviations

CI	Cervical stroma invasion
EC	Endometrial cancer
EEC	Endometrioid endometrial carcinoma
ESMO	European Society for Medical Oncology
FDG	2-[^{18}F]Fluoro-2-deoxy-D-glucose
FIGO	The International Federation of Gynecology and Obstetrics system
LNM	Lymph node metastasis
MI	Myometrial invasion
MRI	Magnetic resonance imaging
NEEC	Non-endometrioid endometrial carcinoma
PACS	Picture Archiving and Communication System
PET/CT	Positron emission tomography computed tomography
SLN	Sentinel lymph node
SUV	Standardized uptake value

Introduction

Endometrial cancer (EC) is one of the most common gynecologic malignancy in high-income countries and the incidence has been rising during the last decades [1, 2]. Most women are diagnosed with localized disease, typically indicating favorable prognosis (5-year survival rates > 95%). However, the high number of new cases (estimated 411,367 annually, worldwide) and the fact that women with advanced disease face less favorable prognosis (5-year survival rates down to 20%) [1, 3, 4] motivate the development of safe and effective diagnostic workups for EC patients.

Standard primary treatment of EC is hysterectomy with bilateral salpingo-oophorectomy allowing surgicopathological staging according to the FIGO system [5]. Depending on presumed risk of advanced stage, recommended surgical lymph node (LN) staging strategy ranges from no LN sampling to sentinel LN mapping (SLN), or lymphadenectomy with resection of pelvic and/or para-aortic LNs [6–8]. Prior to surgery, an endometrial biopsy is typically evaluated and classified into low risk (endometrioid grades 1–2), or high risk (endometrioid grade 3 and non-endometrioid) [6, 7]. However, there are limitations in accuracies for histopathologic evaluation based on biopsies [9, 10]. Furthermore, although preoperative high-risk histology is associated with tumor extension and LN metastases (LNM), 8–10% of low-risk EC still presents with LNM [11].

Pelvic imaging by MRI has over the past decades become widely used for non-invasive preoperative local staging of EC

[12–14]. Whole-body 2-[^{18}F]fluoro-2-deoxy-D-glucose (FDG)-PET/CT has also proven to be useful, especially for detecting LNM and distant spread [15–17]. Although some EC guidelines state that preoperative FDG-PET/CT may be appropriate in patients with high-risk clinical and histologic features [6, 7, 18], FDG-PET/CT is costly and not routinely performed at most centers. However, no studies have systematically investigated the diagnostic value of MRI and FDG-PET/CT in patients with preoperative low-risk versus high-risk histology, nor aimed to define an optimal preoperative imaging workup using MRI combined with selective FDG-PET/CT in EC patients.

In the present study, we hence aim to evaluate the diagnostic performance of MRI and FDG-PET/CT for local staging in EC patients with preoperative low- vs. high-risk histology. In addition, we aim to compare the diagnostic performance for predicting LNM, using four different imaging workups (IWs): MRI in all (IW1), both MRI and FDG-PET/CT in all (IW2), MRI with selective FDG-PET/CT in cases with preoperative high-risk histology (IW3) or MRI with selective FDG-PET/CT in cases with high-risk MRI findings (IW4).

Materials and methods

Patient cohort

This retrospective study included 361 consecutive EC patients diagnosed and treated from October 2011 to July 2019 at the same university hospital (serving a population of ~1 million inhabitants). The diagnosis was established through preoperative biopsy, and histologically verified in hysterectomy specimen. All included patients underwent both pelvic MRI and whole-body FDG-PET/CT with standardized protocols (Table 1) prior to treatment. The images were retrospectively evaluated by radiologists/nuclear medicine physicians who were blinded to clinical information and the original imaging reports. Reference standard was surgicopathological FIGO 2009 stage [5]. Patients diagnosed at our institution during October 2011 to July 2019 that did not have preoperative standardized MRI and/or FDG-PET/CT (*n* = 253), or with missing preoperative histology status (*n* = 11), were not included in the study (supplementary Table S1). This study was conducted under Institutional Review Board (IRB)-approved protocols (IRB approvals 2015/2333; 2015/548; biobank approval 2014/1907) with written informed consent from all patients at primary diagnosis. The consent included approval of prospective collection of clinical patient data, tissue

Table 1 Pelvic MRI and whole-body [18F]FDG-PET/CT acquisition and reconstruction parameters. All scanners are from Siemens

Pelvic MRI:

MRI	Sequence	Plane	TR/TE_1/TE_2 (ms)	FA (Deg)	FOV (mm)	Voxel size (mm)
1.5T Avanto	T2 TSE	AO	6310/95	150	180 × 180	0.9 × 0.7 × 3.0
	T2 TSE	SAG	4920/95	150	180 × 180	0.9 × 0.7 × 3.0
	DWI	AO	3100/79	90	300 × 300	2.3 × 2.3 × 5.0
	T1 VIBE	AO	7.2/2.6	20	250 × 250	1.6 × 1.3 × 2.0
3T Skyra	T2 TSE	AO	4330/94	150	200 × 200	0.5 × 0.5 × 3.0
	T2 TSE	SAG	7360/101	160	200 × 200	0.6 × 0.6 × 3.0
	DWI RESOLVE	AO	6010/74/126	180	200 × 200	1.4 × 1.4 × 3.0
	T1 DIXON	AO	5.9/2.5/3.7	9	250 × 250	1.0 × 1.0 × 1.2

Whole-body [18F]FDG-PET/CT:

PET	Scan time/speed	Corrections	Iteration/subset	Filter	FOV (mm)	Voxel size (mm)
Truepoint	3 min/bed	ATTN/SCAT	4/8	5 mm gauss	700	4.1 × 4.1 × 5.0
Vision	1.1 mm/s	ATTN/SCAT/PSF/TOF	4/5	All pass	700	1.7 × 1.7 × 3.0
CT	**CareDose (ref mAs)**	**CarekV (kV)**	**Recon**	**Filter/IR strength**	**FOV scan/recon (mm)**	**Voxel size (mm)**
Truepoint	Yes (50/240)[a]	No (120)	FB	B19f	500/700	1.4 × 1.4 × 5.0
Vision	Yes (25/210)[a]	Yes (120)	IR	I30f/5	500/780	1.5 × 1.5 × 3.0

AO axial oblique slice orientation, *ATTN* attenuation correction, *Deg* degrees, *DWI* diffusion weighted imaging, *FA* flip angle, *FB* filtered back projection reconstruction, *FOV* field of view, *IR* iterative reconstruction, *PSF* point spread function correction, *RESOLVE* readout segmentation of long variable echo trains, *SCAT* scatter correction, *TE* time echo, *TOF* time of flight correction, *TR* repetition time, *TSE* turbo spin echo, *VIBE* volumetric interpolated breath-hold examination

[a] Reference mAs for low-dose/diagnostic CT protocols

samples, and imaging data (e.g., CT, MRI, PET/CT) from primary diagnostic workup and during follow-ups.

Preoperative endometrial biopsies by pipelle or curettage were histologically classified as endometrioid grades 1–3 (EEC G1–G3), or non-endometrioid endometrial carcinoma (NEEC). Pelvic lymphadenectomy with/without para-aortic lymphadenectomy was routinely performed in all patients with preoperatively defined high-risk disease (NEEC or EEC G3 histology with deep (≥ 50%) myometrial invasion assessed by MRI (MI_{MRI})) according to the European Society of Medical Oncology (ESMO) guidelines [8]. For patients with preoperative low-risk$_{ESMO}$ (EEC G1–G2 with MI_{MRI} < 50%) and intermediate-risk$_{ESMO}$ (EEC G1–G2 with MI_{MRI} ≥ 50%, or EEC G3 with MI_{MRI} < 50%), pelvic lymphadenectomy was selectively omitted if negative imaging findings for LNM and if preserved tumor hormone receptor status (see [19] for further details). Surgical specimens were assessed by pathologists, reporting presence of deep myometrial invasion (MI ≥ 50%), cervical stroma invasion (CI), LNM, and tumor histologic subtype and grade (EEC G1–G3 or NEEC) [20]. Patients were surgically staged according to the FIGO 2009 criteria [5].

Clinical and patient follow-up data were collected from medical records (last accessed 14 September 2021). Progression was defined as local recurrence or progression in the pelvis or new metastases in the abdomen or at distant locations.

MRI scanning

Preoperative pelvic MRI was acquired on a 1.5-T Avanto scanner for 157/361 patients, and on a 3-T Skyra scanner for the remaining 204/361 patients (both Siemens). Prior to imaging, patients were given butylscopolamine bromide intramuscularly/intravenously (20 mg Buscopan, Boehringer Ingelheim), in order to reduce bowel peristalsis. The MRI protocols consisted of contrast-enhanced (CE) axial oblique (perpendicular to the long axis of the uterine body) T1-weighted gradient echo volumetric interpolated breath-hold (VIBE) (1.5T), and VIBE DIXON (3T) images, acquired before and 2 min after administration of contrast agent (0.1 mmol gadolinium/kg body weight) (Fig. 1). Also included in the protocol were sagittal and axial oblique T2-weighted turbo spin echo images, and axial oblique diffusion-weighted images (DWI) with *b*-values of 0 and 1000 s/mm² (1.5T) or 0, 500, and 1000 s/mm² (3T). Protocols at both field strengths (Table 1) were in line with guidelines from the European Society of Urogenital Imaging [12, 13].

MRI reading

All MRI images were de-identified and read independently in PACS by three different readers—in total, eight radiologists with 2–10 years of experience with pelvic MRI. The
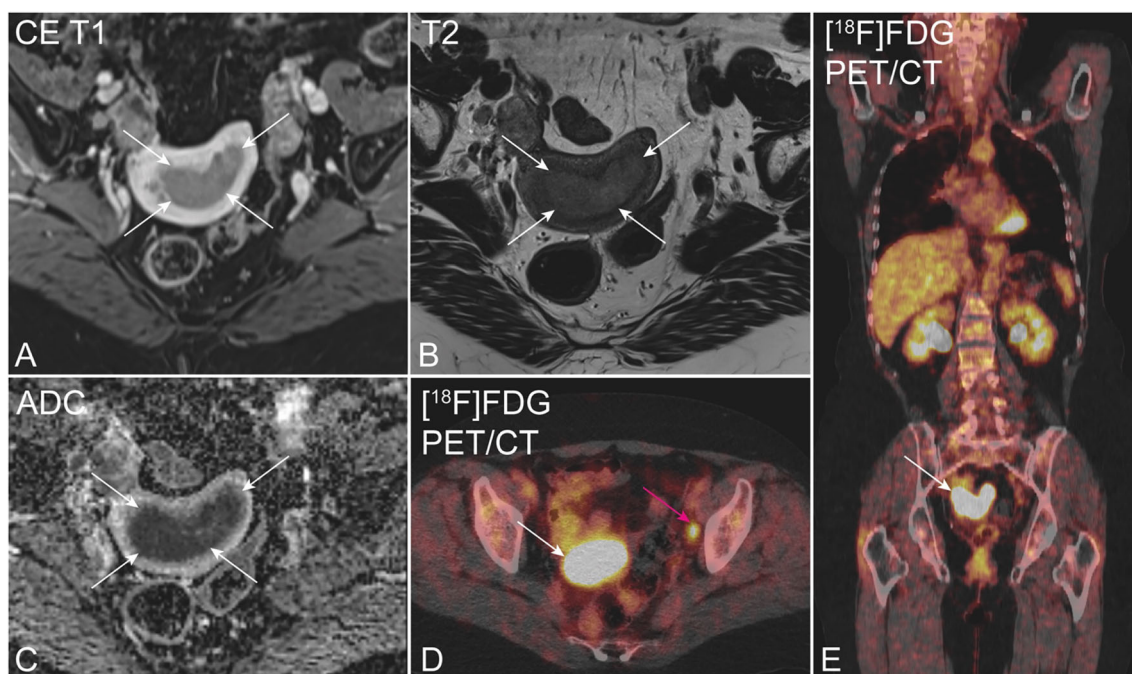
Fig. 1 Preoperative pelvic MRI (**A–C**) and [^{18}F]FDG PET/CT (**D**, **E**) in a 72-year-old patient with endometrial carcinoma, FIGO stage IIIC (endometrioid, grade G1). Axial oblique contrast-enhanced T1-weighted (**A**) and T2-weighted MRI (**B**) depicts an arcuately shaped uterine tumor (white arrows), exhibiting restricted diffusion at apparent diffusion coefficient map (**C**). Axial (**D**) and coronal (**E**) [^{18}F]FDG PET/CT shows elevated [^{18}F]FDG uptake both in the primary tumor (white arrow) and in a left iliac lymph node (cerise arrow)

radiologists were blinded to clinical, pathological, and patient outcome data as well as the MRI report and FDG-PET/CT findings. Myometrial invasion (MI$_{MRI}$: $</\geq$ 50%), cervical stroma invasion (CI$_{MRI}$: yes/no), and enlarged para-aortic or para-iliac LNs (largest LN short-axis diameter LN$_{MRI}$: $</\geq$ 10 mm, irrespective of plane) were recorded separately by all three readers on standardized MRI registration forms. Consensus values were established using the category recorded by the majority of the three readers. Although not reported in the present study, DWI and apparent diffusion coefficient maps were available for the radiologists for visual inspection of (restricted) diffusion in the primary tumor and metastases.

FDG-PET/CT scanning

Preoperative FDG-PET/CT was acquired on a Biograph TruePoint for 325/361 patients and on a Biograph Vision scanner for the remaining 36/361 patients (both Siemens). All patients were instructed to fast for 6 h prior to scanning and FDG was given intravenously approximately 60 min prior to scanning (TruePoint: 370 MBq or 4.6 MBq/kg, Vision: 3 MBq/kg). PET/CT images were acquired from skull base to mid-thigh and PET images were corrected for attenuation and scatter using the CT scan. Further details on PET/CT acquisition and reconstruction are given in Table 1.

FDG-PET/CT reading

All PET images were reviewed on an Oasis workstation (Segami Corporation) by one reader—in total, two nuclear medicine physicians, both with > 4 years of FDG-PET/CT experience. The reader was blinded to clinical, pathological, and patient outcome data as well as the FDG-PET/CT report and MRI findings. Increased FDG uptake (standardized uptake value (SUV) > 2.5) in primary tumor, lymph nodes (LN$_{PET}$: yes/no), and suspected distant metastases (Fig. 1) were recorded in standardized PET registration forms. Finally, PET and the consensus MRI reading were merged with clinical, surgicopathological, and outcome data for further analyses.

Preoperative EC imaging workups (IW1-4) and preoperative risk classification (low, intermediate, and high risk) based on IW4

In order to compare the diagnostic performance metrics for prediction of LNM in EC, four different imaging workups were constructed: IW1, MRI in all patients; IW2, both MRI and FDG-PET/CT in all patients; IW3, MRI with selective FDG-PET/CT in patients with preoperative EEC G3 or NEEC histology; and IW4, MRI with selective FDG-PET/CT in patients with either MI$_{MRI}$ $\geq$ 50%, CI$_{MRI}$, or enlarged LN$_{MRI}$. Detection of LNM were based on either LN$_{MRI}$ alone (IW1) or LN$_{MRI}$ combined with LN$_{PET}$ (IW2-4). Only

patients with surgical LN staging ($n = 220$) were included in these analyses (Table 2, supplementary Table S2).

Applying imaging findings based on IW4, we identified patient groups (Fig. 2A) exhibiting different LNM prevalence (supplementary Figure S1) and survival (supplementary Figure S2), and compared the patient risk

Table 2 Clinical and surgicopathological characteristics in 361 EC patients who underwent preoperative pelvic MRI and [^{18}F]FDG PET/CT and had preoperative histology from biopsy/curettage

Age (median, range)	68 (30, 90)
Preoperative histology[a], *n* (%)	
EEC G1–G2 (low-risk)	240 (66)
EEC G3+NEEC (high-risk)	121 (34)
MI[b], *n* (%)	
< 50%	212 (60)
≥ 50%	144 (40)
CI[b], *n* (%)	
No	308 (86)
Yes	51 (14)
Lymph node surgery, *n* (%)	
No	141 (39)
Yes[c]	220 (61)
LNM[b], *n* (%)	
No	193 (88)
Yes	27 (12)
Histologic subtype[b], *n* (%)	
EEC (G1–G3)	285 (79)
NEEC	76 (21)
Histologic grade (EEC only)[b], *n* (%)	
G1–G2	240 (85)
G3	43 (15)
FIGO stage[b], *n* (%)	
I	283 (78)
II	33 (9)
III	34 (9)
IV	11 (3)
Adjuvant therapy, *n* (%)	
No	230 (64)
Yes[d]	131 (36)

CI cervical stroma invasion, *MI* myometrial invasion, *EEC* endometrioid endometrial carcinoma, *G* grade, *NEEC* non-endometrioid endometrial carcinoma, *FIGO* The International Federation of Gynecology and Obstetrics System, *LNM* lymph node metastases

[a] Based on preoperative biopsy from curettage/pipelle

[b] Based on final histopathology after surgical staging. Missing data (numbers): MI (5), CI (2), histologic grade (2)

[c] Pelvic lymph node sampling in 220/361 patients with accompanying paraaortic lymph node sampling in 79/361 patients

[d] Chemotherapy ($n = 123$), external radiation therapy ($n = 3$), hormonal treatment ($n = 3$), and brachytherapy ($n = 2$).

groups from IW4 with that based in the ESMO risk classification [8] (Fig. 2B). Using IW4, the low-risk$_{IW4}$ group was defined as preoperative EEC G1–G2 histology with either negative MRI findings (for patients with MRI only), or negative LN findings on both MRI and FDG-PET/CT (for patients with both modalities). The intermediate-risk$_{IW4}$ group was defined as either preoperative EEC G1–G2 histology with LN$_{MRI}$ and/or LN$_{PET}$, or preoperative EEC G3+NEEC histology with either negative MRI findings (for patients with MRI only), or negative LN findings on both MRI and FDG-PET/CT. The high-risk$_{IW4}$ group was defined as preoperative EEC G3+NEEC histology with LN$_{MRI}$ and/or LN$_{PET}$ (Fig. 2A).

Statistical analyses

Receiver operating characteristic (ROC) analyses were employed to compare the diagnostic performance of the imaging parameters MI$_{MRI}$, CI$_{MRI}$, LN$_{MRI}$, and LN$_{PET}$ for prediction of surgically assessed MI, CI, and LNM. ROC analyses were also used to assess the different imaging workups' (IW1–4) performance for predicting histologically confirmed LNM. Area under ROC curves (AUCs) were compared using DeLong's test of equality. The Kruskal-Wallis test (with ties) was used to analyze the proposed preoperative risk groups based on IW4 in relation to surgicopathological staging results. The prognostic value of preoperative risk groups based on IW4 and ESMO guidelines was explored using Kaplan-Meier estimator with log-rank test. All statistical analyses were performed with Stata 17.0 (StataCorp).
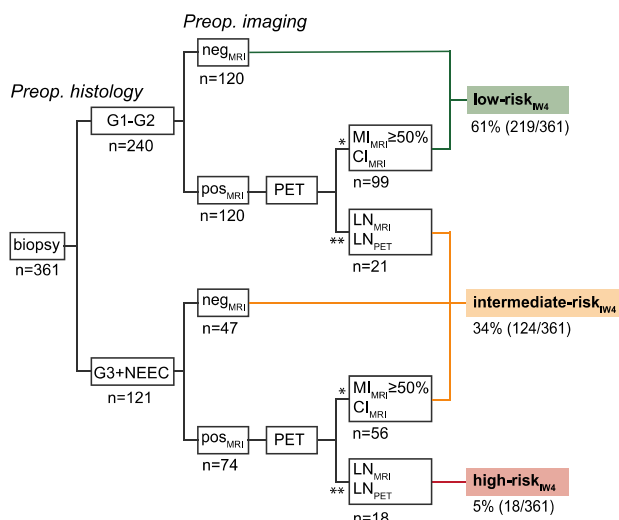
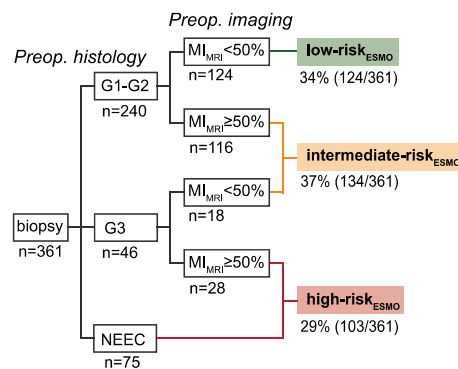## Results

Patients and treatment

During October 2011 to July 2019, a population-based endometrial cancer cohort of 625 consenting patients was prospectively collected at our institution. Of these, 361 patients with preoperative standardized MRI and/or FDG-PET/CT were included in this study, while 264 patients lacking standardized MRI and/or FDG-PET/CT ($n = 253$), or without preoperative histology status ($n = 11$), were excluded. Clinical and surgicopathological characteristics for all included patients ($n = 361$) are given in Table 2. Quite similar surgicopathological patient characteristics were observed in the study cohort ($n = 361$) and the entire patient cohort ($n = 625$, supplementary Table S1).

Primary treatment consisted of hysterectomy with bilateral salpingo-oophorectomy in 98% (355/361) of the patients. These patients were all surgically staged according to FIGO

A) Preoperative risk groups based on imaging workup 4 (IW4)

Preop. imaging

Preop. histology

biopsy n=361

G1-G2 n=240

neg$_{MRI}$ n=120

pos$_{MRI}$ n=120 → PET

* MI$_{MRI}$ ≥50% CI$_{MRI}$ n=99

** LN$_{MRI}$ LN$_{PET}$ n=21

G3+NEEC n=121

neg$_{MRI}$ n=47

pos$_{MRI}$ n=74 → PET

* MI$_{MRI}$ ≥50% CI$_{MRI}$ n=56

** LN$_{MRI}$ LN$_{PET}$ n=18

low-risk$_{IW4}$ 61% (219/361)

intermediate-risk$_{IW4}$ 34% (124/361)

high-risk$_{IW4}$ 5% (18/361)

B) Preoperative risk groups based on ESMO guidelines

Preop. imaging

Preop. histology

biopsy n=361

G1-G2 n=240

MI$_{MRI}$ <50% n=124

MI$_{MRI}$ ≥50% n=116

G3 n=46

MI$_{MRI}$ <50% n=18

MI$_{MRI}$ ≥50% n=28

NEEC n=75

low-risk$_{ESMO}$ 34% (124/361)

intermediate-risk$_{ESMO}$ 37% (134/361)

high-risk$_{ESMO}$ 29% (103/361)

Abbreviations:
G1-3   endometrioid grade 1-3
NEEC   non-endometrioid
MI$_{MRI}$ myometrial invasion on MRI
CI$_{MRI}$ cervical invasion on MRI
LN$_{MRI}$ enlarged pelvic lymph nodes (≥10 mm) on MRI
LN$_{PET}$ lymph nodes with elevated [^{18}F]FDG uptake
neg$_{MRI}$ MI$_{MRI}$ <50%, no CI$_{MRI}$, and no LN$_{MRI}$
pos$_{MRI}$ MI$_{MRI}$ ≥50% and/or CI$_{MRI}$ and/or LN$_{MRI}$

Fig. 2 Preoperative risk groups based on (**A**) imaging workup 4 (IW4), combining preoperative histology and imaging results from MRI and from selective [^{18}F]FDG PET/CT based on MRI findings, and (**B**) the ESMO 2013 clinical practice guidelines for endometrial cancer (EC) in the same EC cohort ($n = 361$). Applying IW4 stratifies 61% of the patients as low-risk, 34% as intermediate-risk, and 5% as high-risk (**A**), whereas the ESMO guidelines stratifies 34% of the patients as low-risk, 37% as intermediate-risk, and 29% as high-risk (**B**). Preoperative histology from curettage/pipelle are classified as endometrioid grades 1–2 (G1–G2), endometrioid grade 3 (G3) or non-endometrioid (NEEC). *This subgroup includes patients with either MI$_{MRI}$ ≥ 50% or CI$_{MRI}$, but negative lymph node findings on both MRI and [^{18}F]FDG PET/CT. **This subgroup includes patients with positive lymph node findings on MRI and/or [^{18}F]FDG PET/CT

2009 staging system (reference standard) [5]. The remaining patients either underwent fertility-sparing treatment ($n = 1$, presumed FIGO I) or tumor debulking surgery ($n = 1$, presumed FIGO IV) or were assessed ineligible for surgery ($n = 4$, presumed FIGO IV). The presumed FIGO stage was based on results from preoperative/operative specimen and diagnostic workup. Pelvic LN surgery was performed in 61% [220/361] of the patients, and 22% [79/361] had accompanying para-aortic lymphadenectomy. Lymphadenectomy was, as expected, more often performed in patients with high-risk preoperative histology (87% [105/121]) compared with patients with low-risk preoperative histology (48% [115/240], supplementary Table S3). Median (range) time span between preoperative imaging and surgical staging was 16 [0–98] days for MRI and 16 [0–89] days for FDG-PET/CT. Median (range) follow-up time was 53 [3–106] months.

MRI and FDG-PET/CT for prediction of surgicopathological MI, CI, and LNM in patients with low-risk vs. high-risk preoperative histology

Diagnostic performance metrics of MI$_{MRI}$, CI$_{MRI}$, LN$_{MRI}$, and LN$_{PET}$ for predicting histopathological MI, CI, and LNM after surgical staging are given in Table 3 for patients with low-risk (EEC G1–G2) and high-risk (EEC G3+NEEC) preoperative histology, respectively. As shown by the similarity in ROC AUC, there were no overall differences in diagnostic performance metrics based on positive MRI and PET findings in patients with low- vs high-risk preoperative histology ($p ≥ 0.16$ for all).

Prediction of LNM by the different imaging workups IW1–4

Prediction of LNM by the four different imaging workups IW1–4 is given in Table 4. IW2 and IW4 yielded highest sensitivities (56% and 52%, respectively), while IW1 and IW3 yielded highest specificities for predicting LNM (95% and 94%, respectively). Furthermore, IW2 and IW4 yielded the highest areas under the ROC curves for prediction of LNM (AUC = 0.73 and 0.72, respectively; Table 4), which were significantly higher or tended to be higher than that of IW1 (AUC = 0.64; $p = 0.04$ and 0.06, respectively, Table 4). IW3 yielded an AUC of 0.69, similar to that of IW1 ($p = 0.13$, Table 4). When comparing the workups including FDG-PET/CT in selected or all cases (IW2–4), no statistically significant differences between the AUCs were observed ($p ≥ 0.24$).

When applying IW4 with selective FDG-PET/CT in patients with high-risk MRI findings, 54% [194/361] would undergo FDG-PET/CT (Fig. 2A), whereas when applying IW3 with selective PET/CT if high-risk preoperative histology, 34% [121/361] of the patients would undergo FDG-PET/CT (Table 2).

Table 3 Performance of preoperative MRI and [18F]FDG PET/CT findings for diagnosing histopathological deep myometrial invasion (MI ≥ 50%), cervical stroma invasion (CI) and lymph node metastases (LNM) for patients preoperatively assessed with low-risk (endometrioid G1–G2) (n = 240) versus high-risk (endometrioid G3 or non-endometrioid (G3+NEEC)) (n = 121) histology (based on biopsy from curettage/pipelle)

Imaging findings[a]	Histopath. findings[b]	Preoperative histology (n)	Sensitivity % (n)	Specificity % (n)	Accuracy % (n)	PPV % (n)	NPV % (n)	ROC AUC (95% ci)	p[c]
$MI_{MRI} \geq 50\%$	MI ≥ 50%	G1–G2 (239)	79 (75/95)	72 (104/144)	75 (179/239)	65 (75/115)	84 (104/124)	0.76 (0.70–0.91)	0.62
		G3+NEEC (117)	82 (40/49)	65 (44/68)	72 (84/117)	63 (40/64)	83 (44/53)	0.73 (0.65–0.81)	
CI_{MRI}	CI	G1–G2 (239)	28 (7/25)	98 (209/214)	90 (216/239)	58 (7/12)	92 (209/227)	0.63 (0.54–0.72)	0.92
		G3+NEEC (120)	31 (8/26)	94 (88/94)	80 (96/120)	57 (8/14)	83 (88/106)	0.62 (0.53–0.72)	
LN_{MRI}	LNM[d]	G1–G2 (115)	40 (4/10)	96 (101/105)	91 (105/115)	50 (4/8)	94 (101/107)	0.68 (0.52–0.84)	0.54
		G3+NEEC (105)	29 (5/17)	94 (83/88)	84 (88/105)	50 (5/10)	87 (83/95)	0.62 (0.50–0.73)	
LN_{PET}	LNM[d]	G1–G2 (115)	70 (7/10)	92 (97/105)	90 (104/115)	47 (7/15)	97 (97/100)	0.81 (0.66–0.96)	0.16
		G3+NEEC (105)	41 (7/17)	93 (82/88)	85 (89/105)	54 (7/13)	89 (82/92)	0.67 (0.55–0.80)	

AUC area under curve, *ci* confidence interval, *CI* cervical stroma invasion, *MI* myometrial invasion, *FIGO* The International Federation of Gynecology and Obstetrics System, *G* grade, *LNM* lymph node metastases, LN_{MRI} enlarged (≥ 10 mm) pelvic lymph node(s) on MRI, LN_{PET} suspicious tracer [18F]FDG uptake in lymph node(s), *NEEC* non-endometrioid endometrial carcinoma, *NPV* negative predictive value, *PPV* positive predictive value, *ROC* receiver operating characteristic curve

[a] Imaging findings based on MRI and [18F]FDG PET/CT

[b] Histopathological findings based on final histopathologic assessment after surgical staging. Missing data (numbers): MI (5), CI (2)

[c] Equality of areas under the ROC curves (AUCs) are assessed by DeLong test

[d] Pelvic lymph node surgery in 220/361 patients

Preoperative EC risk classification based on IW4 compared to ESMO 2013 risk classification

When using IW4, 61% [219/361] of the patients were classified as low-risk$_{IW4}$, 34% [124/361] as intermediate-risk$_{IW4}$, and 5% [18/361] as high-risk$_{IW4}$ (Fig. 2A). Employing the ESMO risk classification in the same patient cohort yielded a lower proportion of patients in the low-risk$_{ESMO}$ group (34% [124/361], Fig. 2B), while a higher proportion of the patients were classified as intermediate- and high-risk$_{ESMO}$ (37% [134/361] and 29% [103/361], respectively, Fig. 2A). The prevalence of LNM was similar in low-risk$_{IW4}$ vs. low-risk$_{ESMO}$ (4% for both, Fig. 3), and in intermediate-risk$_{IW4}$ vs. intermediate-risk$_{ESMO}$ (14% vs. 12%, Fig. 3), while higher in high-risk$_{IW4}$ compared to high-risk$_{ESMO}$ (53% vs. 17%, Fig. 3).

The low-, intermediate-, and high-risk$_{IW4}$ groups exhibited increasing prevalence of both MI ≥ 50%, CI, LNM, high-grade histology, and advanced FIGO stage (III–IV)

Table 4 Prediction of lymph node metastases (LNM) by different imaging workups utilizing pelvic MRI in all (IW1), MRI and [18F]FDG PET/CT in all (IW2), MRI in all and selective [18F]FDG PET/CT in patients preoperatively assessed with high-risk histology (endometrioid grade 3 or non-endometrioid based on biopsy from curettage/pipelle) (IW3), and MRI in all and selective [18F]FDG PET/CT in patients with high-risk MRI-findings (IW4). Only patients with surgical lymph node staging (n = 220) are included in these analyses

Imaging workup	Sensitivity % (n)	Specificity % (n)	Accuracy % (n)	PPV % (n)	NPV % (n)	ROC AUC (95% ci)	p[e]
IW1[a]	33 (9/27)	95 (184/193)	88 (193/220)	50 (9/18)	91 (184/202)	0.64 (0.55–0.74)	
IW2[b]	56 (15/27)	90 (174/193)	86 (189/220)	44 (15/34)	94 (174/186)	0.73 (0.63–0.83)	0.04
IW3[c]	44 (12/27)	94 (181/193)	88 (193/220)	50 (12/24)	92 (181/196)	0.69 (0.59–0.79)	0.13
IW4[d]	52 (14/27)	91 (176/193)	86 (190/220)	45 (14/31)	93 (176/189)	0.72 (0.62–0.81)	0.06

AUC area under curve, *ci* confidence interval, *NPV* negative predictive value, *PPV* positive predictive value, *ROC* receiver operating characteristic curve

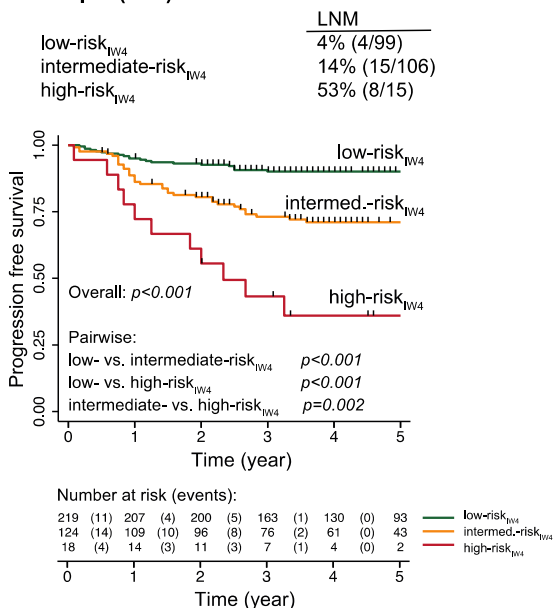[a] Prediction of LNM based on enlarged (≥ 10 mm) pelvic lymph node(s) on MRI (LN_{MRI})

[b] Prediction of LNM based on LN_{MRI} and elevated [18F]FDG uptake in lymph node(s) (LN_{PET}) combined

[c] Prediction of LNM based on LN_{MRI} for patients with low-risk preoperative histology (endometrioid grades 1–2), and LN_{MRI} and LN_{PET} combined for patients with high-risk preoperative histology (endometrioid grade 3 or non-endometrioid)
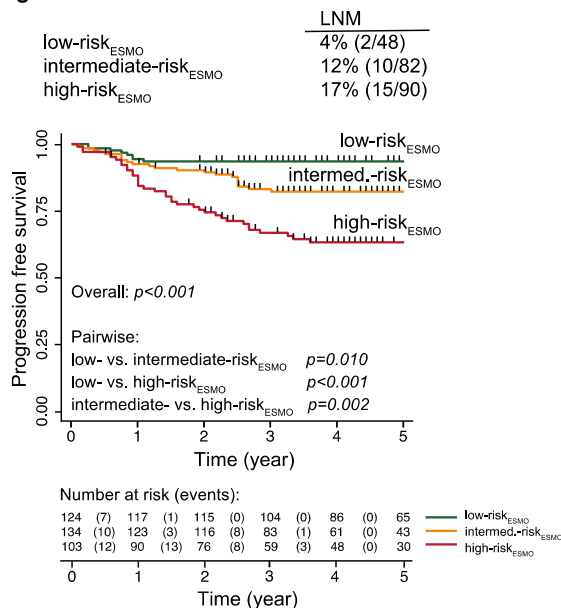
[d] Prediction of LNM based on either LN_{MRI}, or LN_{MRI} and LN_{PET} combined depending on imaging findings on MRI

[e] Equality of AUC between workup 2–4 versus workup 1, assessed by DeLong test

A) Preoperative risk groups based on imaging workup 4 (IW4)

	LNM
low-risk$_{IW4}$	4% (4/99)
intermediate-risk$_{IW4}$	14% (15/106)
high-risk$_{IW4}$	53% (8/15)

Overall: *p<0.001*

Pairwise:
low- vs. intermediate-risk$_{IW4}$	*p<0.001*
low- vs. high-risk$_{IW4}$	*p<0.001*
intermediate- vs. high-risk$_{IW4}$	*p=0.002*

Number at risk (events):
219	(11)	207	(4)	200	(5)	163	(1)	130	(0)	93	low-risk$_{IW4}$
124	(14)	109	(10)	96	(8)	76	(2)	61	(0)	43	intermed.-risk$_{IW4}$
18	(4)	14	(3)	11	(3)	7	(1)	4	(0)	2	high-risk$_{IW4}$

B) Preoperative risk groups based on ESMO guidelines

	LNM
low-risk$_{ESMO}$	4% (2/48)
intermediate-risk$_{ESMO}$	12% (10/82)
high-risk$_{ESMO}$	17% (15/90)

Overall: *p<0.001*

Pairwise:
low- vs. intermediate-risk$_{ESMO}$	*p=0.010*
low- vs. high-risk$_{ESMO}$	*p<0.001*
intermediate- vs. high-risk$_{ESMO}$	*p=0.002*

Number at risk (events):
124	(7)	117	(1)	115	(0)	104	(0)	86	(0)	65	low-risk$_{ESMO}$
134	(10)	123	(3)	116	(8)	83	(1)	61	(0)	43	intermed.-risk$_{ESMO}$
103	(12)	90	(13)	76	(8)	59	(3)	48	(0)	30	high-risk$_{ESMO}$

Fig. 3 Prevalence of lymph node metastases (LNMs) and Kaplan-Meier curves depicting progression-free survival for the preoperative risk groups based on **A** imaging workup 4 (IW4), combining preoperative histology and imaging results from MRI and from selective [^{18}F]FDG PET/CT based on MRI findings, and **B** the ESMO 2013 clinical practice guidelines for endometrial cancer (EC) in the same EC cohort (*n* = 361). *P*-value refers to the Log-Rank test and numbers at risk are given for each time point for the risk groups separately

($p \leq 0.04$ for all, Table 5), and a stepwise reduction in progression-free survival (PFS) for the intermediate- and high-risk$_{IW4}$ groups compared with the low-risk$_{IW4}$ group ($p \leq 0.002$, Fig. 3A). PFS for all of the subgroups within the IW4 categories (Fig. 2A) is presented in supplementary Figure S2.

Discussion

This study presents diagnostic performance metrics for central staging parameters by preoperative MRI and FDG-PET/CT in a large EC cohort, showcasing similar diagnostic performance metrics in patients with low-risk versus high-risk preoperative histology. We further demonstrate that a stepwise approach, utilizing preoperative histology results and MRI in all patients, with selective FDG-PET/CT based on MRI findings, allows classification of patients into preoperative risk groups. Importantly, the risk groups exhibit different prevalence of aggressive surgicopathological features (MI, CI, LNM, high grade, and advanced FIGO stage), and significantly different survival. Furthermore, we show that this stepwise approach, selecting ~54% of the patients to FDG-PET/CT, yields better or similar diagnostic performance metrics for diagnosing LNM, compared to diagnostic imaging workups based on MRI alone or on concurrent MRI and FDG-PET/CT in all.

Pelvic MRI has a pivotal role in locoregional staging of EC [6, 7] and multiple studies have shown that CE MRI yields good diagnostic performance, especially for diagnosing MI $\geq 50\%$ [12, 14, 21]. In a meta-analysis by Wu et al [21], CE MRI had a pooled sensitivity for prediction of MI $\geq 50\%$ of 85% (95% CI: 74–93%). Reported interobserver agreement for radiologists reporting MI $\geq 50\%$ is ranging from fair to very good (κ: 0.32–0.84) [22, 23]. In the present study, we found sensitivities for predicting MI $\geq 50\%$ of 79% (low-risk preoperative histology) and 82% (high-risk preoperative histology), both within the range reported by Wu et al. We also showed that the diagnostic performance metrics of MRI for diagnosing MI $\geq 50\%$, CI, and LNM, were similar in patients with low-risk vs high-risk preoperative histology. Thus, the performance of pelvic MRI seems to be minimally affected by histologic subtype supporting the robustness of MRI for valid preoperative local staging in EC.

The role of FDG-PET/CT in EC imaging is evolving and several studies have shown that FDG-PET/CT compares favorably with conventional MRI for detection of LNM and distant metastases [15, 17, 24, 25]. This is also evident from our study, where MRI only yielded a sensitivity of 33% and an AUC of 0.64 for predicting LNM, while after including FDG-PET/CT in all, the sensitivity and AUC for diagnosing LNM increased to 56% and 0.73, respectively. However, FDG-PET/CT is a costly examination, and access to clinical PET/CT scanning facilities is in many countries limited. Thus, it is important to identify the EC patients that are most likely to benefit from additional FDG-PET/CT as part of their primary diagnostic workup. Several guidelines and previous papers advocate the usage of FDG-PET/CT in patients with

Table 5 Surgicopatological characteristics for the different risk groups defined by the diagnostic workup (IW4) combining preoperative histology and imaging results from MRI and selective [^{18}F]FDG PET/CT based on MRI findings in 361 EC patients

Surgicopathological findings[a] (n)	Low-risk$_{IW4}$ % ($n = 219$)	Intermediate-risk$_{IW4}$ % ($n = 124$)	High-risk$_{IW4}$ % ($n = 18$)	p[b]
MI (356)				0.04
< 50% (212)	63% (138/218)	56% (69/123)	33% (5/15)	
≥ 50% (144)	37% (80/218)	44% (54/123)	67% (10/15)	
CI (359)				< 0.001
No (308)	92% (200/218)	79% (97/123)	61% (11/18)	
Yes (51)	8% (18/218)	21% (26/123)	39% (7/18)	
LNM[c] (220)				< 0.001
No (193)	96% (95/99)	86% (91/106)	47% (7/15)	
Yes (27)	4% (4/99)	14% (15/106)	53% (8/15)	
Histologic subtype (361)				< 0.001
EEC (G1–G3) (285)	99% (216/219)	49% (61/124)	44% (8/18)	
NEEC (76)	1% (3/219)	51% (63/124)	56% (10/18)	
Histologic grade (EEC only) (283)				< 0.001
G1–G2 (240)	97% (207/214)	52% (32/61)	12% (1/8)	
G3 (43)	3% (7/214)	48% (29/61)	88% (7/8)	
FIGO (361)				< 0.001
I–II (316)	95% (209/219)	82% (102/124)	28% (5/18)	
III–IV (45)	5% (10/219)	18% (22/124)	72% (13/18)	

CI cervical stroma invasion, *MI* myometrial invasion, *EEC* endometrioid endometrial carcinoma, *FIGO* The International Federation of Gynecology and Obstetrics System, *G* grade, *NEEC* non-endometrioid endometrial carcinoma, *LNM* lymph node metastases

[a] Based on final histopathologic assessment at surgical staging

[b] Kruskal-Wallis test with ties

[c] Pelvic lymph node surgery in 220/361 patients

Missing data (numbers): MI (5), CI (2), Grade (2)

presumed high risk of advanced FIGO stage, since these are expected to have the highest probability of LNM and distant spread [6, 16–18]. Oxymoronically, the present study failed to show that selective FDG-PET/CT in high-risk patients based on preoperative histology improves the detection of LNM compared to MRI alone (AUC = 0.69 for IW3 vs. AUC = 0.64 for IW1; p = 0.13). It is further evident that including FDG-PET/CT (in addition to MRI) in all patients yields the highest sensitivity (56%) and AUC (0.73) for predicting LNM. However, using an approach with selective FDG-PET/CT based on MRI findings (IW4; sensitivity = 52%, AUC = 0.72) would substantially reduce healthcare costs by only selecting 54% of the patients for FDG-PET/CT, with no significant reduction in diagnostic accuracy compared with that using MRI and FDG-PET/CT in all (IW2).

LN status is one of the main prognostic factors in EC and guides adjuvant treatment [6, 7, 26]. Routine lymphadenectomy in early-stage EC has not been documented to improve outcome and is associated with major comorbidities including lymphedema, lymphocyst formation, and genitofemoral nerve injury [27, 28]. Over the past years, SLN mapping has been introduced as a less-invasive alternative to standard lymphadenectomy in the surgical management of EC. However, SLN mapping requires high surgical expertise, and in a recent survey among gynecological oncologists in Europe and USA, only 50% reported that they used SLN techniques [29]. SLN sampling is also reported to be very challenging in obese patients [30], and leads to increased surgical procedure time and cost compared with that of surgery without lymph node sampling [31]. Thus, preoperative identification of LNM is still essential for optimizing surgical LN staging in patients with LNM, and for safely avoiding invasive staging procedures in patients who do not have LNM (being particularly favorable for patients with comorbidities). Interestingly, the proposed preoperative risk classification using IW4 stratified a higher proportion of patients to low-risk groups (61%) compared to that using the ESMO 2013 classification (34%), however with similar prevalence of LNM (4%) in the low-risk$_{IW4}$ and low-risk$_{ESMO}$ groups. Furthermore, the high-risk$_{IW4}$ group had worse outcome and a higher prevalence of LNM (53%), compared to the high-risk$_{ESMO}$ group (17%).

Several previous EC studies have aimed at predicting LNM by utilizing preoperative molecular biomarkers [11, 32, 33], and a few have also incorporated preoperative imaging findings [34–38]. Reijnen et al have presented a Bayesian network (ENDORISK) that includes molecular and clinical biomarkers, including lymphadenopathy on imaging, yielding AUCs of 0.82–0.84 for predicting LNM [38]. In a study by Berg et al, tumor size measured by MRI was incorporated in a model together with clinical and tumor protein variables, resulting in an AUC of 0.83 for LNM prediction. In the present study, including only preoperative histology and standard imaging findings, the proposed IW4 resulted in a slightly lower AUC of 0.72 for LNM prediction. Although all of the imaging workups (IW1–4) yielded high specificities (90–95%) and NPVs (91–94%) for LNM detection, their relatively low sensitivities (33–56%) and PPVs (44–50%) show that conventional staging information based on preoperative EC imaging has clear limitations. However, several promising functional and structural imaging markers have been reported in EC that may be combined with conventional imaging markers to improve the staging performance of MRI and FDG-PET/CT [14]. For MRI, tumor markers from diffusion-weighted imaging (DWI) [23, 39], dynamic contrast-enhanced MRI [40], tumor size/volume [15, 41], and MRI radiomics [42, 43] have all been reported to predict surgicopathological stage and outcome in EC. For FDG-PET/CT, large metabolic tumor volume [15, 44] and specific PET radiomics features [45] have also been linked to markers of aggressive disease and poor outcome in EC. How information from histological, molecular, and clinical examinations should be combined with tumor information retrieved from conventional and advanced diagnostic imaging in order to yield even better prediction of LNM and outcome in EC should be further explored and validated in independent patient cohorts in future studies.

Limitations

Lymphadenectomy is, at most sites, omitted in patients with clinical and histological low risk of LNM in order to limit post-surgical side effects. In the present study, lymphadenectomy was performed in only 48% of patients with low-risk preoperative histology versus 87% of the patients with high-risk preoperative histology. This may potentially have introduced an inherent selection bias in the analyses of diagnostic performance metrics for detecting LNM among patients subjected to lymphadenectomy ($n = 220$). This limitation is, however, hard to avoid, as it would be considered unethical to perform LN sampling routinely in low-risk patients who would be unlikely to benefit from this invasive surgical procedure.

Conclusion

In this large EC study, we evaluated the diagnostic performance metrics for central staging parameters by preoperative MRI and FDG-PET/CT in subgroups with low-risk versus high-risk preoperative histology—finding similar diagnostic performance in the low- and high-risk histology groups. Furthermore, we propose a stepwise imaging workup incorporating information about preoperative MRI findings that selected ~54% of the patients to FDG-PET/CT. This workup yielded high diagnostic performance for prediction of LNM and identified preoperative EC risk groups exhibiting significantly different risks of advanced disease and poor outcome. The proposed stepwise imaging workup represents a promising approach to ensure preoperative image-guided risk stratification and LNM detection in EC, while avoiding unnecessary use of FDG-PET/CT in patients who are less likely to benefit from a costly FDG-PET/CT examination.

Declarations

Guarantor The scientific guarantor of this publication is Ingfrid S. Haldorsen.

Conflict of interest The authors of this manuscript declare no relationships with any companies, whose products or services may be related to the subject matter of the article.

Statistics and biometry One of the authors has significant statistical expertise.

Informed consent Written informed consent was obtained at primary diagnosis from all patients in this retrospective study on prospectively collected data.

Ethical approval Institutional Review Board approval was obtained.

Study subjects or cohort overlap Some study subjects have been previously reported in:

1. Fasmer KE, Gulati A, Dybvik JA, et al (2020) Preoperative 18F-FDG PET/CT tumor markers outperform MRI-based markers for the prediction of lymph node metastases in primary endometrial cancer. Eur Radiol 30:2443–2453. 10.1007/s00330-019-06622-w

2. Ytre-Hauge S, Husby JA, Magnussen IJ, et al (2015) Preoperative tumor size at MRI predicts deep myometrial invasion, lymph node

metastases, and patient outcome in endometrial carcinomas. Int J Gynecol Cancer 25:459–466. 10.1097/IGC.0000000000000367

3. Husby JA, Reitan BC, Biermann M, et al (2015) Metabolic Tumor Volume on 18F-FDG PET/CT Improves Preoperative Identification of High-Risk Endometrial Carcinoma Patients. J Nucl Med 56:1191–1198. 10.2967/jnumed.115.159913

Methodology
• retrospective
• observational
• performed at one institution

References

1. Sung H, Ferlay J, Siegel RL et al (2021) Global Cancer Statistics 2020: GLOBOCAN estimates of incidence and mortality worldwide for 36 cancers in 185 countries. CA Cancer J Clin 71:209–249. https://doi.org/10.3322/caac.21660

2. Lu KH, Broaddus RR (2020) Endometrial cancer. N Engl J Med 383:2053–2064. https://doi.org/10.1056/NEJMra1514010

3. Cancer Registry of Norway (2019) Cancer in Norway 2018 - cancer incidence, mortality, survival and prevalence in Norway. Cancer Registry of Norway

4. Cancer of the Endometrium - Cancer Stat Facts. In: SEER. https://seer.cancer.gov/statfacts/html/corp.html. Accessed 6 Jul 2021

5. Pecorelli S (2009) Revised FIGO staging for carcinoma of the vulva, cervix, and endometrium. Int J Gynaecol Obstet 105:103–104

6. Colombo N, Creutzberg C, Amant F et al (2015) ESMO-ESGO-ESTRO consensus conference on endometrial cancer: diagnosis, treatment and follow-up. Radiother Oncol 117:559–581. https://doi.org/10.1016/j.radonc.2015.11.013

7. Concin N, Matias-Guiu X, Vergote I et al (2021) ESGO/ESTRO/ESP guidelines for the management of patients with endometrial carcinoma. Int J Gynecol Cancer 31:12–39. https://doi.org/10.1136/ijgc-2020-002230

8. Colombo N, Preti E, Landoni F et al (2013) Endometrial cancer: ESMO Clinical Practice Guidelines for diagnosis, treatment and follow-up. Ann Oncol 24:vi33–vi38. https://doi.org/10.1093/annonc/mdt353

9. Visser NCM, Reijnen C, Massuger LFAG et al (2017) Accuracy of endometrial sampling in endometrial carcinoma: a systematic review and meta-analysis. Obstet Gynecol 130:803–813. https://doi.org/10.1097/AOG.0000000000002261

10. Helpman L, Kupets R, Covens A et al (2014) Assessment of endometrial sampling as a predictor of final surgical pathology in endometrial cancer. Br J Cancer 110:609–615. https://doi.org/10.1038/bjc.2013.766

11. Trovik J, Wik E, Werner HMJ et al (2013) Hormone receptor loss in endometrial carcinoma curettage predicts lymph node metastasis and poor outcome in prospective multicentre trial. Eur J Cancer 49:3431–3441. https://doi.org/10.1016/j.ejca.2013.06.016

12. Nougaret S, Horta M, Sala E et al (2019) Endometrial cancer MRI staging: updated guidelines of the European Society of Urogenital Radiology. Eur Radiol 29:792–805. https://doi.org/10.1007/s00330-018-5515-y

13. Kinkel K, Forstner R, Danza FM et al (2009) Staging of endometrial cancer with MRI: guidelines of the European Society of Urogenital Imaging. Eur Radiol 19:1565–1574. https://doi.org/10.1007/s00330-009-1309-6

14. Haldorsen IS, Salvesen HB (2016) What is the best preoperative imaging for endometrial cancer? Curr Oncol Rep 18:25. https://doi.org/10.1007/s11912-016-0506-0

15. Fasmer KE, Gulati A, Dybvik JA et al (2020) Preoperative 18F-FDG PET/CT tumor markers outperform MRI-based markers for the prediction of lymph node metastases in primary endometrial cancer. Eur Radiol 30:2443–2453. https://doi.org/10.1007/s00330-019-06622-w

16. Atri M, Zhang Z, Dehdashti F et al (2017) Utility of PET/CT to evaluate retroperitoneal lymph node metastasis in high-risk endometrial cancer: results of ACRIN 6671/GOG 0233 Trial. Radiology 283:450–459. https://doi.org/10.1148/radiol.2016160200

17. Gee MS, Atri M, Bandos AI et al (2018) Identification of distant metastatic disease in uterine cervical and endometrial cancers with FDG PET/CT: analysis from the ACRIN 6671/GOG 0233 Multicenter Trial. Radiology 287:176–184. https://doi.org/10.1148/radiol.2017170963

18. ACR Appropriateness Criteria® Pretreatment evaluation and follow-up of endometrial cancer | Elsevier Enhanced Reader. https://reader.elsevier.com/reader/sd/pii/S1546144020309388?token=8B59E17F517AEB672CE890CC79E898A3B19624D9BDCE130FE87D6159007532 85EC02B263A9F38D1CA62831AD9A4525AD&originRegion=eu-west-1&originCreation=20210423092844. Accessed 23 Apr 2021

19. Forsse D, Berg HF, Bozickovic O et al (2021) Maintained survival outcome after reducing lymphadenectomy rates and optimizing adjuvant treatment in endometrial cancer. Gynecol Oncol 160:396–404. https://doi.org/10.1016/j.ygyno.2020.12.002

20. Soslow RA, Tornos C, Park KJ et al (2019) Endometrial carcinoma diagnosis: use of FIGO grading and genomic subcategories in clinical practice: recommendations of the International Society of Gynecological Pathologists. Int J Gynecol Pathol 38(Suppl 1):S64–S74. https://doi.org/10.1097/PGP.0000000000000518

21. Wu L-M, Xu J-R, Gu H-Y et al (2013) Predictive value of T2-weighted imaging and contrast-enhanced MR imaging in assessing myometrial invasion in endometrial cancer: a pooled analysis of prospective studies. Eur Radiol 23:435–449. https://doi.org/10.1007/s00330-012-2609-9

22. Haldorsen IS, Husby JA, Werner HMJ et al (2012) Standard 1.5-T MRI of endometrial carcinomas: modest agreement between radiologists. Eur Radiol 22:1601–1611. https://doi.org/10.1007/s00330-012-2400-y

23. Husby JA, Salvesen OO, Magnussen IJ et al (2015) Tumour apparent diffusion coefficient is associated with depth of myometrial invasion and is negatively correlated to tumour volume in endometrial carcinomas. Clin Radiol 70:487–494

24. Kim HJ, Cho A, Yun M et al (2016) Comparison of FDG PET/CT and MRI in lymph node staging of endometrial cancer. Ann Nucl Med 30:104–113. https://doi.org/10.1007/s12149-015-1037-8

25. Bollineni VR, Ytre-Hauge S, Bollineni-Balabay O et al (2016) High diagnostic value of 18F-FDG PET/CT in endometrial cancer: systematic review and meta-analysis of the literature. J Nucl Med 57:879–885. https://doi.org/10.2967/jnumed.115.170597

26. Brooks RA, Fleming GF, Lastra RR et al (2019) Current recommendations and recent progress in endometrial cancer. CA Cancer J Clin 69:258–279. https://doi.org/10.3322/caac.21561

27. Abu-Rustum NR, Alektiar K, Iasonos A et al (2006) The incidence of symptomatic lower-extremity lymphedema following treatment of uterine corpus malignancies: a 12-year experience at Memorial Sloan-Kettering Cancer Center. Gynecol Oncol 103:714–718. https://doi.org/10.1016/j.ygyno.2006.03.055

28. Cardosi RJ, Cox CS, Hoffman MS (2002) Postoperative neuropathies after major pelvic surgery. Obstet Gynecol 100:240–244. https://doi.org/10.1016/S0029-7844(02)02052-5

29. Casarin J, Multinu F, Abu-Rustum N et al (2019) Factors influencing the adoption of the sentinel lymph node technique for endometrial cancer staging: an international survey of gynecologic oncologists. Int J Gynecol Cancer 29:60–67. https://doi.org/10.1136/ijgc-2018-000020

30. Eriksson AGZ, Montovano M, Beavis A et al (2016) Impact of obesity on sentinel lymph node mapping in patients with newly diagnosed uterine cancer undergoing robotic surgery. Ann Surg Oncol 23:2522–2528. https://doi.org/10.1245/s10434-016-5134-2

31. Geppert B, Lönnerfors C, Bollino M, Persson J (2018) Sentinel lymph node biopsy in endometrial cancer-feasibility, safety and lymphatic complications. Gynecol Oncol 148:491–498. https://doi.org/10.1016/j.ygyno.2017.12.017

32. Tangen IL, Kopperud RK, Visser NC et al (2017) Expression of L1CAM in curettage or high L1CAM level in preoperative blood samples predicts lymph node metastases and poor outcome in endometrial cancer patients. Br J Cancer 117:840–847. https://doi.org/10.1038/bjc.2017.235

33. Fonnes T, Trovik J, Edqvist P-H et al (2018) Asparaginase-like protein 1 expression in curettage independently predicts lymph node metastasis in endometrial carcinoma: a multicentre study. BJOG 125:1695–1703. https://doi.org/10.1111/1471-0528.15403

34. Berg HF, Ju Z, Myrvold M et al (2020) Development of prediction models for lymph node metastasis in endometrioid endometrial carcinoma. Br J Cancer 122:1014–1022. https://doi.org/10.1038/s41416-020-0745-6

35. Kang S, Kang WD, Chung HH et al (2012) Preoperative identification of a low-risk group for lymph node metastasis in endometrial cancer: a Korean gynecologic oncology group study. J Clin Oncol 30:1329–1334. https://doi.org/10.1200/jco.2011.38.2416

36. Todo Y, Sakuragi N, Nishida R et al (2003) Combined use of magnetic resonance imaging, CA 125 assay, histologic type, and histologic grade in the prediction of lymph node metastasis in endometrial carcinoma. Am J Obstet Gynecol 188:1265–1272

37. Lee JY, Jung DC, Park SH et al (2010) Preoperative prediction model of lymph node metastasis in endometrial cancer. Int J Gynecol Cancer 20:1350–1355. https://doi.org/10.1111/IGC.0b013e3181f44f5a

38. Reijnen C, Gogou E, Visser NCM et al (2020) Preoperative risk stratification in endometrial cancer (ENDORISK) by a Bayesian network model: A development and validation study. PLoS Med 17:e1003111. https://doi.org/10.1371/journal.pmed.1003111

39. Nakamura K, Imafuku N, Nishida T et al (2012) Measurement of the minimum apparent diffusion coefficient (ADCmin) of the primary tumor and CA125 are predictive of disease recurrence for patients with endometrial cancer. Gynecol Oncol 124:335–339

40. Fasmer KE, Bjørnerud A, Ytre-Hauge S et al (2018) Preoperative quantitative dynamic contrast-enhanced MRI and diffusion-weighted imaging predict aggressive disease in endometrial cancer. Acta Radiol 59:1010–1017. https://doi.org/10.1177/0284185117740932

41. Ytre-Hauge S, Husby JA, Magnussen IJ et al (2015) Preoperative tumor size at MRI predicts deep myometrial invasion, lymph node metastases, and patient outcome in endometrial carcinomas. Int J Gynecol Cancer 25:459–466. https://doi.org/10.1097/IGC.0000000000000367

42. Fasmer KE, Hodneland E, Dybvik JA et al (2021) Whole-volume tumor MRI radiomics for prognostic modeling in endometrial cancer. J Magn Reson Imaging. https://doi.org/10.1002/jmri.27444

43. Ytre-Hauge S, Dybvik JA, Lundervold A et al (2018) Preoperative tumor texture analysis on MRI predicts high-risk disease and reduced survival in endometrial cancer. J Magn Reson Imaging 48:1637–1647. https://doi.org/10.1002/jmri.26184

44. Shim S-H, Kim D-Y, Lee D-Y et al (2014) Metabolic tumour volume and total lesion glycolysis, measured using preoperative 18F–FDG PET/CT, predict the recurrence of endometrial cancer. BJOG Int J Obstet Gynaecol 121:1097–1106. https://doi.org/10.1111/1471-0528.12543

45. Wang T, Sun H, Guo Y, Zou L (2019) 18F-FDG PET/CT quantitative parameters and texture analysis effectively differentiate endometrial precancerous lesion and early-stage carcinoma. Mol Imaging 18:1536012119856965. https://doi.org/10.1177/1536012119856965